tert-Butylazapentadienyl–Iridium–Phosphine Chemistry[1]

John R. Bleeke,* Scott T. Luaders, and Kerry D. Robinson

Department of Chemistry, Washington University, St. Louis, Missouri 63130

Received October 25, 1993®

Potassium *tert*-butylazapentadienide reacts with (Cl)Ir(PMe_3)$_3$ to produce (*syn*-(1,2,3-η)-5-*tert*-butyl-5-azapentadienyl)Ir(PMe_3)$_3$ (**1a**). Treatment of **1a** with acetone leads to attack at the central allylic carbon of the azapentadienyl ligand (C2) and production of a novel iridacyclobutane complex, **2**. The X-ray crystal structure of **2** (monoclinic, $C2/c$, a = 31.117(6) Å, b = 11.104(2) Å, c = 18.457(5) Å, β = 119.26(2)°, V = 5563(2) Å^3, Z = 8, R = 0.033, R_w = 0.042) shows the expected *trans* orientation of the imine and acetone substituents on the four-membered ring. When **1a** is stirred in pentane solution, it gradually converts to the thermodynamically favored *anti*-η^3-azapentadienyl isomer, **1b**. The structure of **1b** has been confirmed by X-ray crystallography (monoclinic, $P2_1/n$, a = 15.709(14) Å, b = 26.154(10) Å, c = 18.915(7) Å, β = 108.97(3)°, V = 7351(3) Å^3, Z = 12, R = 0.053, R_w = 0.069). The relatively short C3–C4 bond distance (1.449(26) Å) in the azapentadienyl ligand of **1b** may reflect some contribution by an η^4-butadiene resonance structure. Treatment of **1b** with triflic acid results in clean protonation of the nitrogen center and production of [(η^4-(*tert*-butylamino)butadiene)Ir(PMe_3)$_3$]$^+O_3SCF_3^-$ (**3**). Addition of a second equivalent of triflic acid results in a second protonation at nitrogen, generating the dicationic species **5**. Treatment of **1a** with 1 or 2 equiv of triflic acid also leads primarily to formation of **3** and **5**, respectively. However, a side reaction (~20%) involving protonation at iridium also occurs, generating (*syn*-η^3-*tert*-butylazapentadienyl)Ir(PMe_3)$_3$(H)$^+$-$O_3SCF_3^-$ (**4**) and [(*syn*-η^3-CH_2–CH–CHCH=NHC(CH_3)$_3$)Ir(PMe_3)$_3$(H)]$^{2+}$($O_3SCF_3^-$)$_2$ (**6**), respectively. Compounds **1a**, **1b** and **3** are fluxional in solution, due to facile rotation of the π ligands with respect to the Ir(PMe_3)$_3$ fragment. NMR line-shape analysis has yielded rotational barriers ($\Delta G^\ddagger$) of 11.5(4), 11.1(4), and 16.4(4) kcal/mol, respectively.

Introduction

During the past decade, transition-metal complexes containing the acyclic pentadienyl ligand have been extensively investigated.[2] In contrast, relatively little effort has been directed toward synthesizing and studying the chemistry of (heteropentadienyl)metal complexes, *i.e.*, species in which one atom of the pentadienyl ligand chain has been replaced with a heteroatom.[3] Like their pentadienyl analogues, these complexes promise to exhibit a variety of ligand bonding modes and a rich reaction chemistry based on facile ligand rearrangements.

Recently, we have initiated a systematic synthetic study of (heteropentadienyl)metal complexes, using halo–metal–phosphine compounds and anionic heteropentadienide reagents as our building blocks. Previous papers have reported the reactions of halo–iridium–phosphine compounds with oxapentadienide,[1b] thiapentadienide,[1c] and phosphapentadienide[1a] reagents. We now describe results of a parallel study involving (Cl)Ir(PMe_3)$_3$ and the nitrogen-containing heteropentadienide reagent, potassium *tert*-butylazapentadienide.

Scheme 1

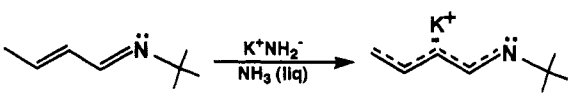

Results and Discussion

A. Reaction of (Cl)Ir(PMe_3)$_3$ with Potassium *tert*-Butylazapentadienide. Synthesis of (*syn*-η^3-*tert*-butylazapentadienyl)Ir(PMe_3)$_3$ (1a). As shown in Scheme 1, potassium *tert*-butylazapentadienide can be synthesized by reacting *tert*-butylazapentadiene with potassium amide in liquid ammonia. The NMR spectra of this species are identical with those reported in 1991 be Würthwein[4] for the lithium analogue and are consistent with its formulation as the *E,E* isomer. Treatment of (Cl)-Ir(PMe_3)$_3$ with potassium *tert*-butylazapentadienide in tetrahydrofuran leads to the immediate formation of (*syn*-(1,2,3-η)-5-*tert*-butyl-5-azapentadienyl)Ir(PMe_3)$_3$ (**1a**) (see Scheme 2). This reaction involves nucleophilic attack by the *carbon* end of the *tert*-butylazapentadienide reagent and, in this way, differs from analogous reactions involving oxapentadienide ($C_4H_5O^-$),[1b] thiapentadienide ($C_4H_5S^-$),[1c] and phosphapentadienide ($C_4H_5PH^-$)[1a] reagents, where attack by the *heteroatom* is observed. Most likely, this reversal in the site of reaction results from the presence of the bulky *tert*-butyl substituent on nitrogen rather than from a decrease in the nucleophilicity of the heteroatom.

The ^{1}H NMR spectrum of **1a** shows the expected pattern of resonances. The imine hydrogen (H4) resonates farthest

® Abstract published in *Advance ACS Abstracts*, April 1, 1994.

(1) Pentadienyl–Metal–Phosphine Chemistry. 27. Previous papers in this series include: (a) Bleeke, J. R.; Rohde, A. M.; Robinson, K. D. *Organometallics* **1994**, *13*, 401. (b) Bleeke, J. R.; Haile, T.; New, P. R.; Chiang, M. Y. *Organometallics* **1993**, *12*, 517. (c) Bleeke, J. R.; Ortwerth, M. F.; Chiang, M. Y. *Organometallics* **1992**, *11*, 2740.

(2) For leading reviews, see: (a) Ernst, R. D. *Chem. Rev.* **1988**, *88*, 1251. (b) Yasuda, H.; Nakamura, A. *J. Organomet. Chem.* **1985**, *285*, 15. (c) Powell, P. *Adv. Organomet. Chem.* **1986**, *26*, 125.

(3) To our knowledge, only one previous example of an (azapentadienyl)metal complex has been isolated: Cheng, M.-H.; Cheng, C.-Y.; Wang, S.-L.; Peng, S.-M.; Liu, R.-S. *Organometallics* **1990**, *9*, 1853.

(4) Wolf, G.; Würthwein, E.-U. *Chem. Ber.* **1991**, *124*, 889.

0276-7333/94/2313-1592$04.50/0

Scheme 2

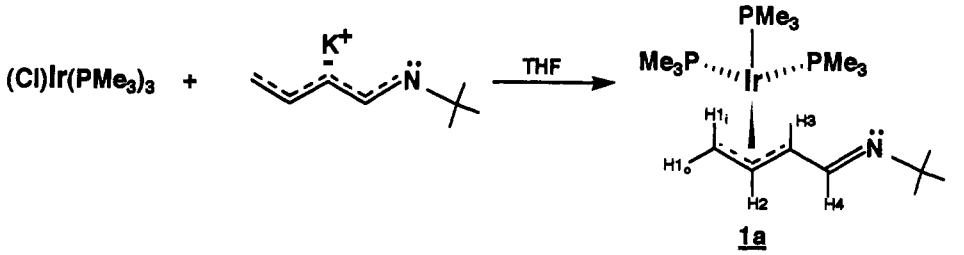

Scheme 3

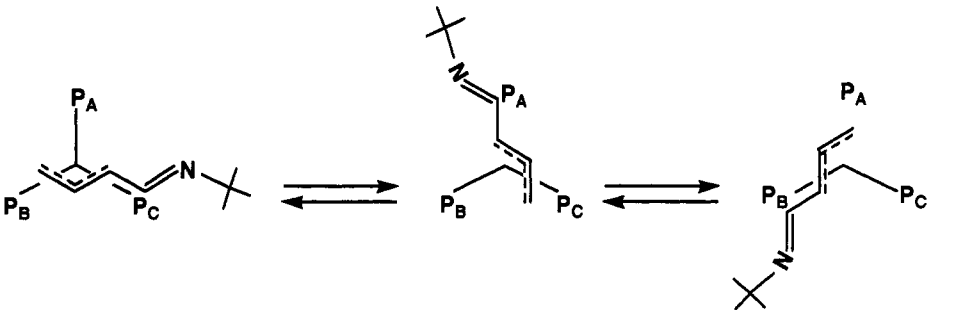

downfield (at δ 7.41) and appears as a doublet due to coupling to H3 (J_{H4-H3} = 9.3 Hz), while allylic hydrogens H2, H3, $H1_{outer}$, and $H1_{inner}$ resonate at δ 4.27, 2.17, 1.30, and 0.14, respectively. All are multiplets due to proton and phosphorus coupling. In the $^{13}C\{^1H\}$ NMR spectrum, imine carbon C4 appears at δ 164.5, while allylic carbons C2, C3, and C1 resonate at δ 54.6, 42.5, and 19.3, respectively. The signals for C1 and C3 appear as quartets (J = 7.5 Hz) due to coupling to three equivalent ^{31}P nuclei. This equivalence of the ^{31}P nuclei, which also manifests itself in the $^{31}P\{^1H\}$ NMR spectrum (a singlet at 25 °C), is apparently due to rapid rotation of the η^3-azapentadienyl ligand with respect to the $Ir(PMe_3)_3$ fragment.[5] Under this process, the three phosphine ligands take turns beneath the "open mouth" of the η^3-azapentadienyl ligand (Scheme 3). However, as the compound is cooled to −90 °C, the exchange process is stopped, and the $^{31}P\{^1H\}$ spectrum decoalesces to three independent signals. NMR line-shape analysis has established a free energy of activation ($\Delta G^{\ddagger}$) of 11.5 ± 0.4 kcal/mol for this rotational process. In the infrared spectrum of **1a**, the imine C=N stretch appears at 1621 cm^{-1}.

B. Synthesis and Structure of a Novel Acetone Adduct, 2. Compound **1a** crystallizes readily from pentane at −30 °C, and a single-crystal X-ray diffraction study has confirmed the postulated structure. However, poor crystal quality and the extreme X-ray sensitivity of **1a** has prevented high-precision determination of bond distances and angles. Attempts to crystallize **1a** from acetone led instead to the formation of a novel acetone adduct, iridacyclobutane complex **2** (see Scheme 4). This reaction apparently involves attack by acetone (perhaps in the enol form) on the central allylic carbon (C2) of the η^3-azapentadienyl ligand in **1a**. One of the acetone hydrogens ultimately ends up on the iridium center as a hydride ligand. This hydrogen transfer step could be catalyzed by trace water in the acetone (water does cocrystallize with **2**; *vide infra*) or even by the imine nitrogen. Although nucleophiles usually add to the

Scheme 4

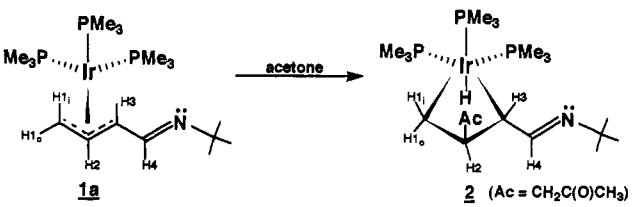

terminal carbon of an η^3-allyl ligand, other additions to the central carbon have been observed in electron-rich systems.[6] The remarkable feature of this reaction is the ease with which it occurs, given the weakly nucleophilic character of acetone.

The NMR data for **2** are fully consistent with the postulated structure. In particular, the $^{31}P\{^1H\}$ NMR shows an ABC pattern characteristic of octahedral *fac*-tris(phosphine) complexes. In the ^1H NMR, the metal hydride appears as a double of triplets due to large coupling to the *trans* phosphine and smaller coupling to the two *cis* phosphines. Imine hydrogen H4 still resonates far downfield (δ 7.36) and retains its coupling to H3, while the metallacyclic ring protons (H1's, H2, and H3) all shift upfield from their positions in **1a**, as expected for hydrogens bonded to sp^3 carbons. Similarly, in the $^{13}C\{^1H\}$ NMR spectrum, C1, C2, and C3 shift upfield relative to their positions in **1a**, and C1 and C3 exhibit large *trans*-phosphorus couplings (J_{C-P} = 61.6 Hz). The infrared spectrum of **2** shows three strong peaks in the 1600–2000-cm^{-1} region: the imine C=N stretch at 1611 cm^{-1}, the acetone C=O stretch at 1699 cm^{-1} and the iridium hydride stretch at 1972 cm^{-1}. When **2** is synthesized using acetone-d_6, the hydride resonance in the ^1H NMR and the metal hydride stretch in the IR disappear.

The structure of **2** has been confirmed by X-ray crystallography (see ORTEP drawing, Figure 1). Positional parameters and bond distances and angles are given in Tables 1 and 2. The coordination geometry about

(5) Rotational barriers for η^3-allyl ligands are typically quite low. See: Mingos, D. M. P. In *Comprehensive Organometallic Chemistry*; Pergamon: Oxford, England, 1982; Vol. 3, pp 60–67.

(6) See, for example: (a) Ephretikine, M.; Francis, B. R.; Green, M. L. H.; Mackenzie, R. E.; Smith, M. J. *J. Chem. Soc., Dalton Trans.* **1977**, 1131. (b) Periana, R. A.; Bergman, R. G. *J. Am. Chem. Soc.* **1984**, *106*, 7272.

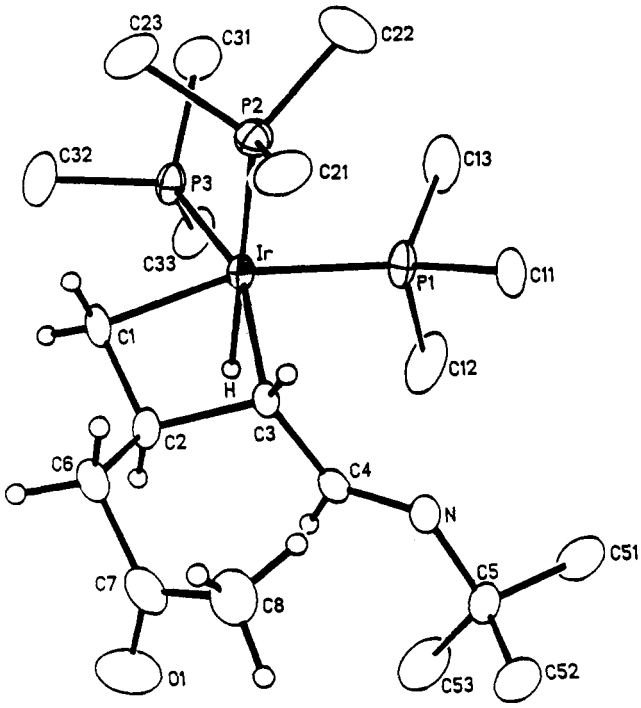

Figure 1. ORTEP drawing of *fac*-$CH_2CH(CH_2C(O)CH_3)CH(CHNC(CH_3)_3)Ir(PMe_3)_3(H)\cdot{}^1/_2H_2O$ (**2**).

Table 1. Atomic Coordinates ($\times10^4$) with Estimated Standard Deviations for Non-Hydrogen Atoms in *fac*-$CH_2CH(CH_2C(O)CH_3)CH(CHNC(CH_3)_3Ir(PMe_3)_3(H)\cdot{}^1/_2H_2O$ (2)

	x	*y*	*z*
Ir	3498(1)	86(1)	2496(1)
P1	3428(1)	−184(3)	1204(1)
P2	4209(1)	−1049(2)	3271(2)
P3	2928(1)	−1336(3)	2362(2)
O1	3908(4)	4855(8)	3722(8)
O2[a]	5000	1867(10)	2500
N	4037(2)	3062(6)	1853(4)
C1	3594(3)	885(9)	3629(5)
C2	3733(3)	2108(8)	3432(5)
C3	3904(3)	1786(8)	2801(5)
C4	3772(3)	2688(8)	2155(5)
C5	3882(4)	4008(9)	1217(6)
C51	3853(6)	3466(10)	463(7)
C52	4292(5)	4936(9)	1553(8)
C53	3398(5)	4634(12)	1015(9)
C6	4098(4)	2850(9)	4194(5)
C7	4211(5)	4045(11)	3961(7)
C8	4686(4)	4197(11)	3952(7)
C11	3970(4)	164(9)	1108(6)
C12	2968(4)	796(14)	414(6)
C13	3248(5)	−1627(12)	652(7)
C21	4800(3)	−247(9)	3792(7)
C22	4357(5)	−2297(11)	2800(8)
C23	4236(4)	−1865(11)	4146(7)
C31	3009(5)	−2930(9)	2260(8)
C32	2773(4)	−1372(12)	3194(6)
C33	2320(4)	−1105(11)	1471(6)

[a] O2 is the oxygen atom of the $^1/_2$ H_2O.

iridium is a distorted octahedron in which the three phosphine phosphorus atoms, the hydride hydrogen atom, and ring carbon atoms C1 and C3 occupy the six coordination sites. The largest deviation from idealized octahedral geometry involves the angle C1–Ir–C3, whose small value (66.8(4)°) is, of course, dictated by the constraints of the metallacyclobutane ring. The four-membered ring exhibits some puckering, with a dihedral

Table 2. Selected Bond Distances (Å) and Bond Angles (deg) with Estimated Standard Deviations for *fac*-$CH_2CH(CH_2C(O)CH_3)CH(CHNC(CH_3)_3Ir(PMe_3)_3(H)\cdot{}^1/_2H_2O$ (2)

Bond Distances			
Ir-P1	2.306(3)	C4-N	1.271(14)
Ir-P2	2.333(2)	N-C5	1.471(12)
Ir-P3	2.295(3)	C2-C6	1.544(11)
Ir-C1	2.155(10)	C6-C7	1.489(17)
Ir-C3	2.187(8)	C7-C8	1.497(21)
C1-C2	1.523(14)	C7-O1	1.218(16)
C2-C3	1.540(16)	O2-N	2.943(9)[a]
C3-C4	1.455(12)		
Bond Angles			
P1-Ir-P2	98.3(1)	C2-C3-Ir	91.5(6)
P1-Ir-P3	97.0(1)	Ir-C3-C4	119.1(5)
P2-Ir-P3	98.4(1)	C2-C3-C4	113.4(8)
P1-Ir-C1	162.9(3)	C3-C4-N	126.9(8)
P1-Ir-C3	97.4(3)	C4-N-C5	123.5(8)
P2-Ir-C1	89.3(2)	C1-C2-C6	115.3(7)
P2-Ir-C3	93.0(2)	C3-C2-C6	116.1(9)
P3-Ir-C1	97.0(3)	C2-C6-C7	112.6(8)
P3-Ir-C3	160.1(3)	C6-C7-C8	118.5(10)
C1-Ir-C3	66.8(4)	C6-C7-O1	120.9(13)
Ir-C1-C2	93.2(6)	C8-C7-O1	120.4(13)
C1-C2-C3	102.6(8)		

[a] O2 is the oxygen atom of the $^1/_2$ H_2O.

angle of 25.8° between the plane C1–Ir–C3 and the plane C1–C2–C3. Hydrogen atoms H2 and H3 reside on opposite sides of the ring. This orientation requires that in the reacting species (**1a**) the η^3-azapentadienyl ligand must possess a "syn" (W-shaped) geometry, in which H2 and H3 are situated *anti* to one another (see Scheme 4). The stereochemistry about the imine double bond is *trans*; the torsion angle C3–C4–N–C5 is 178.0°. Interestingly, the solid-state structure of **2** contains $^1/_2$ equiv of water. Each water molecule in the unit cell resides on a crystallographic 2-fold rotation axis and is hydrogen-bonded to two imine nitrogens, as evidenced by an O–N distance of 2.943(9) Å.[7]

C. Synthesis and Structure of (*anti*-η^3-*tert*-butylazapentadienyl)Ir(PMe$_3$)$_3$ (1b). When **1a** is stirred in pentane solution, it gradually converts to the thermodynamically favored *anti*-η^3-azapentadienyl isomer, **1b**; the conversion is ~90% complete in 1 h at 25 °C. Several mechanisms for this transformation can be envisaged. One possibility, shown in Scheme 5, involves the intermediacy of 3-η-azapentadienyl species in which rotation about C2–C3 is facile.[8] Alternatively, direct rotation about C2–C3 may be possible, particularly if the η^4-*s*-*trans*-butadiene resonance structure contributes to the bonding in **1a**. Note

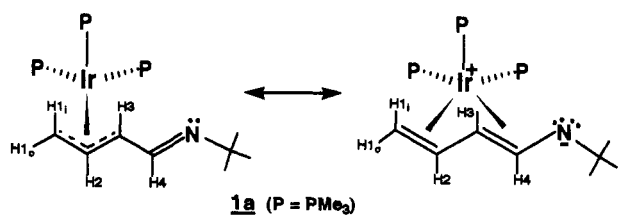

1a (P = PMe$_3$)

that in this resonance structure, the formal negative charge resides on the most electronegative atom, nitrogen, while

(7) Stout, G. H.; Jensen, L. H. *X-Ray Structure Determination, A Practical Guide*; Macmillan: New York, 1968; p 303.

(8) Similar $\eta^3 \rightarrow \eta^1$ isomerizations are common in (allyl)metal chemistry: Collman, J. P.; Hegedus, L. S.; Norton, J. R.; Finke, R. G. *Principles and Applications of Organometallic Chemistry*; University Science Books: Mill Valley, CA, 1987; pp 175–181.

Scheme 5

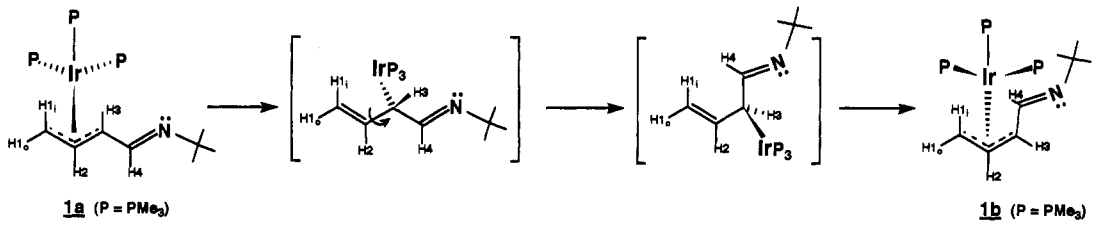

Table 3. Atomic Coordinates (×10⁴) with Estimated Standard Deviations for Non-Hydrogen Atoms in (*anti*-η³-*tert*-butylazapentadienyl)Ir(PMe₃)₃ (1b)

	x	*y*	*z*		*x*	*y*	*z*
			Molecule 1				
Ir1	2070(1)	−1209(1)	4098(1)	C32	−38(11)	−801(8)	2963(14)
P1	3407(3)	−820(2)	4222(3)	C33	1342(14)	−158(9)	2813(15)
P2	1663(3)	−799(2)	5008(3)	C1a	1179(12)	−1884(6)	3830(11)
P3	1167(3)	−810(2)	3063(3)	C2a	2059(13)	−1975(6)	3814(9)
C11	3545(16)	−141(7)	4087(18)	C3a	2783(11)	−1938(5)	4549(9)
C12	4267(13)	−917(10)	5122(13)	C4a	2683(11)	−2101(5)	5249(9)
C13	3987(13)	−1078(9)	3593(13)	N5a	3358(9)	−2220(6)	5816(8)
C21	1394(15)	−111(7)	4930(14)	C6a	3221(12)	−2384(8)	6504(11)
C22	2460(15)	−817(10)	5960(11)	C7a	3758(17)	−2023(10)	7096(12)
C23	653(13)	−1028(9)	5166(13)	C8a	2293(13)	−2469(10)	6489(12)
C31	1142(16)	−1119(10)	2182(11)	C9a	3692(16)	−2908(10)	6648(14)
			Molecule 2				
Ir2	2097(1)	5675(1)	4783(1)	C62	−93(11)	5870(9)	3616(14)
P4	3316(3)	5960(2)	4500(3)	C63	1152(15)	6320(11)	3028(14)
P5	1905(3)	4885(2)	4236(3)	C1b	1244(11)	5663(7)	5475(10)
P6	1052(3)	6143(2)	3924(3)	C2b	2092(12)	5903(5)	5820(10)
C41	3515(15)	6644(7)	4498(15)	C3b	2855(12)	5565(6)	5986(8)
C42	4397(12)	5750(11)	5106(15)	C4b	2877(11)	5055(6)	6266(9)
C43	3456(14)	5786(9)	3615(12)	N5b	3604(9)	4808(6)	6587(8)
C51	2910(12)	4470(7)	4474(13)	C6b	3563(11)	4290(7)	6896(10)
C52	1077(13)	4477(7)	4451(13)	C7b	2624(12)	4099(8)	6833(13)
C53	1505(14)	4809(8)	3207(10)	C8b	4128(14)	4343(9)	7732(13)
C61	866(15)	6778(8)	4275(15)	C9b	4034(18)	3937(9)	6534(16)
			Molecule 3				
Ir3	2230(1)	1957(1)	4409(1)	C92	1279(19)	2009(11)	2505(12)
P7	3556(3)	2328(2)	4459(3)	C93	120(12)	2326(8)	3247(14)
P8	1874(3)	2403(2)	5315(3)	C1c	1407(18)	1282(7)	4239(13)
P9	1314(3)	2325(2)	3363(3)	C2c	2240(16)	1192(7)	4190(16)
C71	4052(16)	2115(12)	3787(16)	C3c	2905(13)	1253(5)	4933(10)
C72	3694(14)	3011(8)	4439(17)	C4c	2814(11)	1126(5)	5662(10)
C73	4496(12)	2209(10)	5315(13)	N5c	3489(10)	1044(5)	6227(9)
C81	2814(15)	2480(8)	6217(11)	C6c	3381(14)	909(8)	6951(10)
C82	1501(15)	3066(8)	5162(14)	C7c	2446(13)	913(11)	6990(13)
C83	967(14)	2146(7)	5606(13)	C8c	3994(19)	1270(9)	7525(12)
C91	1432(16)	2996(9)	3125(14)	C9c	3790(17)	374(8)	7171(14)

the formal positive charge is localized on iridium, where it can be effectively neutralized by the PMe_3 ligands.

The thermodynamic preference for the *anti* isomer may result from resonance stabilization provided by the η^4-*s*-*cis*-butadiene structure. In all likelihood, this structure is

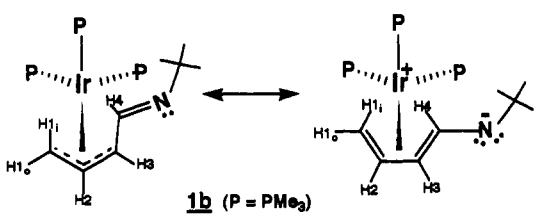

an even more important contributor to the bonding in **1b** than the corresponding *s*-*trans*-butadiene resonance structure is to **1a**. Evidence for this resonance structure comes from the X-ray crystal structure of **1b** (*vide infra*), where bond length C3–C4 is found to be significantly shorter than a normal C–C single bond. Similar structural features have been observed in an (*anti*-η^3-oxapentadienyl)metal complex[1b] and in (*anti*-η^3-pentadienyl)metal complexes.[9]

Further supporting the η^4-*s*-*cis*-butadiene resonance structure is the observed decrease in the frequency of the imine C=N stretch in the IR spectrum. In **1b**, this bond appears at 1607 cm^{-1}, as compared to 1621 cm^{-1} in the *syn* isomer, **1a**.

The ^1H and $^{13}C\{^1H\}$ NMR spectra for **1b** closely resemble those for **1a**, with the only major difference being a substantial downfield shift for allyllic proton H3 (to δ 3.89 in **1b** from δ 2.17 in **1a**). This deshielding of H3 is typical for (*anti*-η^3-allyl)metal complexes. Like **1a**, compound **1b** is fluxional at room temperature; rapid rotation of the η^3-azapentadienyl ligand about the iridium–allyl axis causes the three PMe_3 ligands to appear equivalent in the room-temperature $^{31}P\{^1H\}$ NMR spectrum. However, cooling the sample to −90 °C results in a decoalescence to three doublet of doublet patterns. NMR line-shape analysis yields a ΔG^* value of 11.1 ± 0.4 kcal/mol for this rotational process.

(9) (a) Bleeke, J. R.; Donaldson, A. J.; Peng, W.-J. *Organometallics* **1988**, *7*, 33. (b) Lee, G.-H.; Peng, S.-M.; Liu, F.-C.; Mu, D.; Liu, R.-S. *Organometallics* **1989**, *8*, 402.

Table 4. Selected Bond Distances (Å) and Bond Angles (deg) with Estimated Standard Deviations for (*anti*-η^3-*tert*-butylazapentadienyl)Ir(PMe_3)$_3$ (1b)

molecule 1		molecule 2		molecule 3	
		Bond Distances			
Ir1–P1	2.278(5)	Ir2–P4	2.275(5)	Ir3–P7	2.273(5)
Ir1–P2	2.290(6)	Ir2–P5	2.287(5)	Ir3–P8	2.290(6)
Ir1–P3	2.263(5)	Ir2–P6	2.258(4)	Ir3–P9	2.249(5)
Ir1–C1a	2.205(16)	Ir2–C1b	2.156(21)	Ir3–C1c	2.149(22)
Ir1–C2a	2.073(15)	Ir2–C2b	2.052(20)	Ir3–C2c	2.043(19)
Ir1–C3a	2.235(14)	Ir2–C3b	2.217(14)	Ir3–C3c	2.194(14)
C1a–C2a	1.411(28)	C1b–C2b	1.424(23)	C1c–C2c	1.360(40)
C2a–C3a	1.486(21)	C2b–C3b	1.439(24)	C2c–C3c	1.461(29)
C3a–C4a	1.448(26)	C3b–C4b	1.433(23)	C3c–C4c	1.470(29)
C4a–N5a	1.277(19)	C4b–N5b	1.280(20)	C4c–N5c	1.256(20)
N5a–C6a	1.452(27)	N5b–C6b	1.487(24)	N5c–C6c	1.478(28)
		Bond Angles			
P1–Ir1–P2	100.7(2)	P4–Ir2–P5	100.8(2)	P7–Ir3–P8	101.2(2)
P1–Ir1–P3	100.3(2)	P4–Ir2–P6	97.0(2)	P7–Ir3–P9	99.7(2)
P2–Ir1–P3	100.6(2)	P5–Ir2–P6	101.9(2)	P8–Ir3–P9	101.4(2)
P1–Ir1–C1a	151.2(5)	P4–Ir2–C1b	152.2(5)	P7–Ir3–C1c	148.9(8)
P1–Ir1–C3a	90.7(5)	P4–Ir2–C3b	94.2(5)	P7–Ir3–C3c	92.2(5)
P2–Ir1–C1a	103.6(6)	P5–Ir2–C1b	104.2(5)	P8–Ir3–C1c	104.4(8)
P2–Ir1–C3a	109.9(5)	P5–Ir2–C3b	107.1(4)	P8–Ir3–C3c	106.8(5)
P3–Ir1–C1a	90.0(5)	P6–Ir2–C1b	89.7(5)	P9–Ir3–C1c	92.3(6)
P3–Ir1–C3a	145.0(4)	P6–Ir2–C3b	146.2(5)	P9–Ir3–C3c	146.5(5)
C1a–Ir1–C3a	66.8(6)	C1b–Ir2–C3b	66.9(6)	C1c–Ir3–C3c	63.7(7)
C1a–C2a–C3a	115.1(17)	C1b–C2b–C3b	114.6(13)	C1c–C2c–C3c	108.6(24)
C2a–C3a–C4a	123.9(16)	C2b–C3b–C4b	124.9(17)	C2c–C3c–C4c	128.3(19)
C3a–C4a–N5a	122.1(17)	C3b–C4b–N5b	123.8(16)	C3c–C4c–N5c	121.6(18)
C4a–N5a–C6a	120.0(16)	C4b–N5b–C6b	120.1(15)	C4c–N5c–C6c	120.7(17)

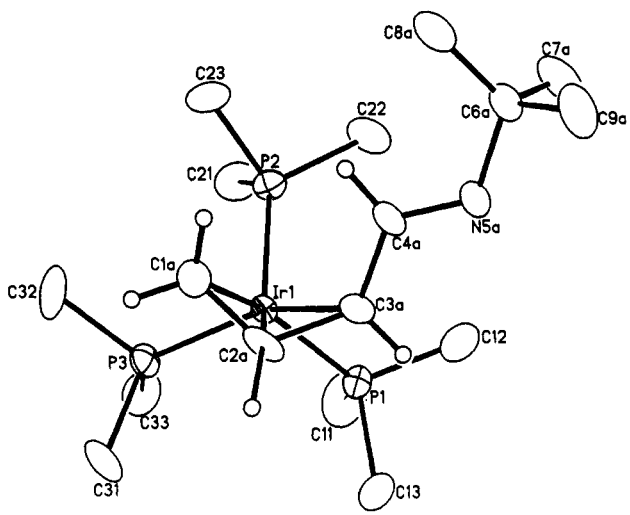

Figure 2. ORTEP drawing of (*anti*-η^3-*tert*-butylazapentadienyl)Ir(PMe_3)$_3$ (**1b**). One of the three crystallographically independent molecules is pictured.

Crystals of **1b** were grown from a saturated pentane solution at −30 °C, and the solid-state structure was determined by X-ray crystallography. The compound crystallized with three independent molecules in the asymmetric unit. The ORTEP drawing of one of these is shown in Figure 2, while positional parameters and bond distances and angles are given in Tables 3 and 4, respectively. As expected, the azapentadienyl ligand has the *anti* geometry (torsional angle C1–C2–C3–C4 = 36.9°).[10] However, *trans* stereochemistry prevails throughout the rest of the ligand with torsional angles C2–C3–C4–N5 and C3–C4–N5–C6 having values of 158.6 and 178.4°, respectively.[10] As is common for *anti*-η^3-pentadienyl ligands, the imine moiety is bent out of the plane of the allyl moiety.[9,11] Hence, atoms C4 and N5 lie 0.71 and 1.01 Å, respectively, out of the C1/C2/C3 plane and the dihedral angle between planes C1/C2/C3 and C3/C4/N5 is 29.4°.[10] Perhaps the most interesting structural feature of the molecule is the C3–C4 bond distance of 1.449(26) Å, which is significantly shorter than a normal C–C single bond. By comparison, the two allylic bonds, C1–C2 and C2–C3, have lengths of 1.401(30) and 1.462(25) Å, respectively.[10] As discussed earlier, the short C3–C4 bond may reflect some contribution by an η^4-butadiene structure to the overall bonding picture in **1b**.

Scheme 6

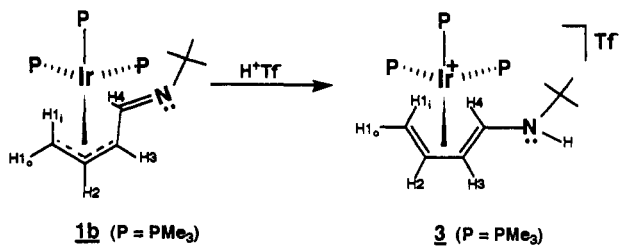

Unlike its *syn* isomer, compound **1b** is completely unreactive toward acetone, presumably because the nucleophilic addition in this case would place the bulky acetone and imine substituents on the same side of the four-membered ring in the developing product. Furthermore, unlike the closely related oxapentadienyl complex (*anti*-η^3-oxapentadienyl)Ir(PMe_3)$_3$, **1b** shows no tendency to undergo C4–H4 bond activation to generate a metallacyclic product.[1b] The problem with this reaction is apparently unfavorable steric contacts between the imine *tert*-butyl group and the phosphine ligands in the developing octahedral product.

D. Protonation of Compounds 1b and 1a. Synthesis of Cationic Complexes 3 and 4. As shown in Scheme 6,

(10) These numbers represent averages of the three crystallographically independent molecules.

(11) Chardon, C.; Eisenstein, O.; Johnson, T.; Caulton, K. G. *New J. Chem.* **1992**, *16*, 781. Note: This reference also contains a good discussion of the factors contributing to the relatively high rotational barrier in diene–iridium–phosphine systems.

Scheme 7

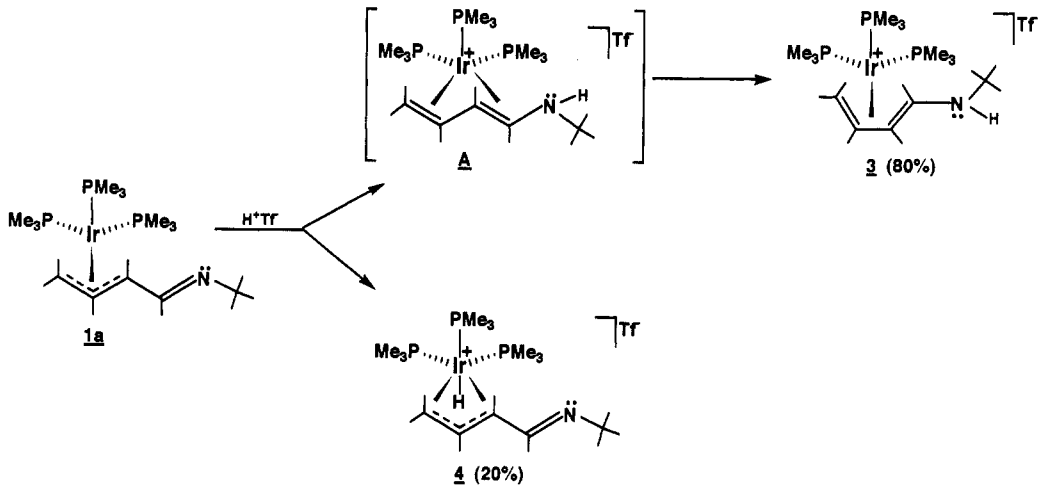

treatment of **1b** with triflic acid leads to protonation at nitrogen and clean formation of η^4-(*tert*-butylamino)-butadiene complex **3**. Perhaps the most striking feature of the ^{1}H NMR spectrum for **3**, as compared to those for **1a,b** and **2**, is the disappearance of the downfield imine proton, H4; it appears at δ 2.38 in **3**. Similarly, in the ^{13}C{^{1}H} NMR spectrum, imine carbon C4 is shifted upfield to δ 65.9. The amino N–H proton resonance in **3** is obscured by the intense methyl peaks of the PMe_3 ligands and the *tert*-butyl group; however, it can be detected in the 2D COSY spectrum (at δ 1.02) by virtue of its coupling to H4. At 25 °C, the NMR spectra for **3** indicate that the phosphine ligands are slowly exchanging, due to rotation of the η^4-(*tert*-butylamino)butadiene ligand about the butadiene–iridium axis. In particular, three broad resonances are seen in the room-temperature ^{31}P{^{1}H} NMR spectrum. These signals coalesce upon heating to 100 °C and resolve into three separate, well-defined resonances upon cooling to −25 °C. Line-shape analysis indicates a $\Delta G^{\ddagger}$ for this rotational process of 16.4 ± 0.4 kcal/mol. This rotational barrier, while higher than that observed in many other d^8 (η^4-diene)ML_3 complexes, appears to be in line with analogous $[(\eta^4\text{-diene})Ir(PR_3)_3]^+$ systems.[11]

Treatment of (*syn*-η^3-*tert*-butylazapentadienyl)$Ir(PMe_3)_3$ (**1a**) with triflic acid also leads to formation of **3**, presumably through the intermediacy of the transient *s-trans*-(*tert*-butylamino)butadiene complex (**A**; Scheme 7).[12] However, this process is accompanied by a side reaction (~20%) involving protonation at the iridium center to form the iridium hydride species (**4**; Scheme 7). In the ^{1}H NMR of **4**, the hydride resonates at δ −15.17 and is split into a doublet ($J_{H\text{-trans-}P}$ = 129.4 Hz) of triplets ($J_{H\text{-cis-}P's}$ = 17.1 Hz) by the PMe_3 ligands. H4 resonates in the imine region of the spectrum (δ 7.38), confirming the η^3-bonding mode for the azapentadienyl ligand. Compound **4** does not convert to **3** upon stirring at room temperature.[13]

E. Protonation of Compounds 3 and 4. Synthesis of Dicationic Complexes 5 and 6. As shown in Scheme 8, treatment of **3** with a second equivalent of triflic acid leads to a second protonation at nitrogen and production of compound **5**. The NMR spectra of **5** closely resemble those of **3**, although the N–H resonances are shifted far downfield (to δ 7.40 and 7.25), as expected for an ammonium salt. Compound **5** is less soluble in organic solvents than **3**, but it does dissolve sparingly in solvents such as acetone and methylene chloride. Unlike compound **3**, **5** is not fluxional. At 25 °C, ^{1}H, ^{13}C{^{1}H}, and ^{31}P{^{1}H} NMR spectra all exhibit sharp peaks in the PMe_3 regions, and no appreciable broadening is observed upon heating to 100 °C. The conversion of **3** to **5** is readily reversible. Hence, treatment of **5** with bases such as lithium diisopropylamide leads to the immediate reformation of **3**. In fact, treatment of **5** with 1 equiv of **1b** cleanly produces 2 equiv of **3** (see Scheme 9).

Scheme 8

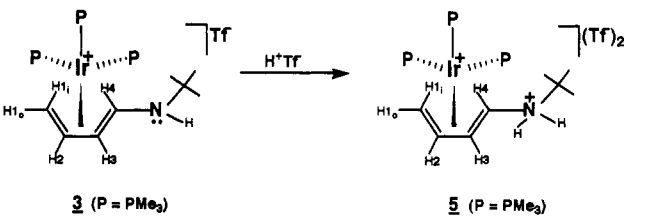

Treatment of the 80/20 mixture of **3** and **4**, derived from protonation of **1a** (Scheme 7), with an additional 1 equiv of triflic acid leads to an 80/20 mixture of compound **5** (*vide supra*) and compound **6**, in which both iridium and nitrogen are singly protonated (see Scheme 10). The ^{1}H NMR spectrum of **6** is qualitatively similar to that of **4**, clearly indicating the presence of a metal hydride and an η^3-bound azapentadienyl ligand. The hydride signal shifts downfield to δ −13.9 but still appears as a doublet of triplets due to phosphorus coupling, while proton H4 moves downfield to δ 8.4. The iminium N–H proton is observed as a broad singlet at δ 11.7. Interestingly, the protonated η^3-*tert*-butylazapentadienyl ligand in **6** does not rearrange to an η^4-(*tert*-butylamino)butadiene structure, perhaps because such a rearrangement would require placing a formal dipositive charge at the iridium center. Furthermore, compound **6** does not convert to **5**, even upon prolonged stirring at room temperature.[14] If less than 1 equiv of triflic acid is added to the 80/20 mixture of **3** and

(12) While similar (*s-trans*-1,3-diene)metal intermediates have recently been observed in protonation reactions involving (η^3-oxapentadienyl)-metal and (η^3-pentadienyl)metal complexes (see references below), low-temperature NMR monitoring of our system did not detect signals due to **A**. For M = Mo, see: (a) Benyunes, S. A.; Green, M.; Grimshire, M. J. *Organometallics* **1989**, *8*, 2268. (b) Benyunes, S. A.; Binelli, A.; Green, M.; Grimshire, M. J. *J. Chem. Soc., Dalton Trans.* **1991**, 895. For M = Ru, see: (c) Benyunes, S. A.; Day, J. P.; Green, M.; Al-Saadoon, A. W.; Waring, T. L. *Angew. Chem., Int. Ed. Engl.* **1990**, *29*, 1416.

(13) However, a second set of peaks, consistent with the *anti* isomer of **4**, does appear in the NMR after many hours of stirring.

(14) However, another set of peaks, consistent with the *anti* isomer of **6**, does appear in the NMR upon prolonged stirring.

Scheme 9

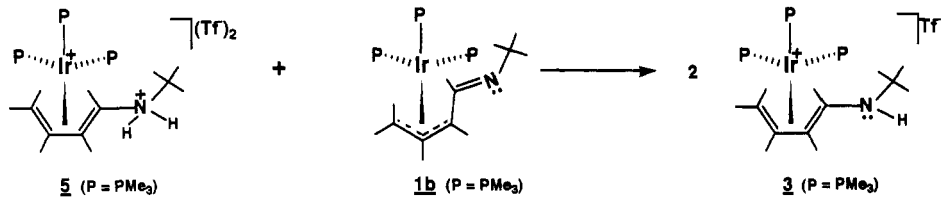

Scheme 10

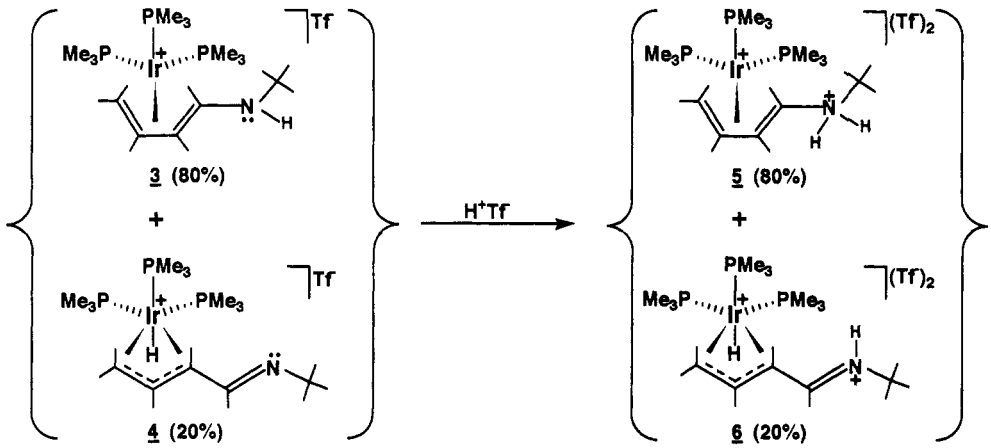

4, compound 4 is preferentially protonated. This "competition experiment" indicates that the imine nitrogen atom in 4 is more basic than the amine nitrogen center in 3.

Conclusion

The work reported herein represents the first rational synthesis of (azapentadienyl)metal complexes using an anionic reagent as the source of the azapentadienyl ligand. While the chemistry bears some similarity to that of related (pentadienyl)metal[15] and (heteropentadienyl)metal[1] systems, the nitrogen atom exerts its influence in a variety of ways. For example, the electronegativity of the nitrogen center stabilizes the η^4-butadiene resonance structure, which in turn leads to a preference for the *anti*-η^3-azapentadienyl bonding mode over the isomeric *syn*-η^3 mode. The basicity of the nitrogen atom leads to nitrogen-centered protonations and the production of amino-substituted (butadiene)metal complexes. Further investigations of (azapentadienyl)metal complexes are planned.

Experimental Section

General Comments. All manipulations were carried out under a nitrogen atmosphere, using either glovebox or double-manifold Schlenk techniques. Solvents were stored under nitrogen after being distilled from the appropriate drying agents. Diethyl ether and tetrahydrofuran were dried over sodium/benzophenone, pentane was dried over calcium hydride, and acetone was dried over magnesium sulfate. The following reagents were obtained from the supplier indicated and used without further purification: anhydrous ammonia (Matheson), potassium (Aldrich), crotonaldehyde (Aldrich), *tert*-butylamine (Aldrich), $IrCl_3 \cdot 3H_2O$ (Johnson-Matthey), cyclooctene (Aldrich), trimethylphosphine (Strem), and triflic acid (Aldrich). *tert*-Butylazapentadiene[16] and $[(cyclooctene)_2IrCl]_2$[17] were prepared using literature procedures.

NMR experiments were performed on a Varian XL-300 or Varian VXR-500 NMR spectrometer. ^1H and ^{13}C spectra were referenced to tetramethylsilane, while ^{31}P spectra were referenced to external H_3PO_4. In general, ^1H connectivities were determined from COSY (^1H–^1H correlation spectroscopy) spectra; HMQC (^1H-detected multiple quantum coherence) and APT (attached proton test) experiments aided in assigning some of the ^1H and ^{13}C peaks. Note: In all of the NMR spectra, carbon atoms and associated hydrogen are numbered by *starting* at the end of the chain *opposite nitrogen*.

The infrared spectra were recorded on a Mattson Polaris FT IR spectrometer. Microanalyses were performed by Galbraith Laboratories, Inc., Knoxville, TN.

Synthesis of Potassium *tert*-Butylazapentadienide. To 250 mL of liquid ammonia at −78 °C was added a small piece of potassium metal. After the appearance of a blue color, a few crystals of ferric nitrate (~0.1 g) were added, followed by small pieces of potassium until a total of 3.9 g (0.10 mol) had been added. After this mixture had been stirred for 2 h at −78 °C, *tert*-butylazapentadiene (12.5 g, 0.10 mol) was added dropwise over a period of 1 h. The resultant solution was then stirred at −78 °C for an additional 1 h and slowly warmed to room temperature, during which time the ammonia evaporated off. To complete the removal of ammonia, the residue was placed under vacuum for 1 h. After extraction with tetrahydrofuran and filtration through Celite, the red-brown solution was evacuated to dryness, yielding potassium *tert*-butylazapentadienide as a brick red solid: yield 13.9 g, 85%. The NMR spectra for this reagent were identical with those reported earlier earlier for the lithium salt.[4]

Synthesis of (*syn*-η^3-*tert*-butylazapentadienyl)Ir(PMe$_3$)$_3$ (1a). At 25 °C, trimethylphosphine (0.26 g, 3.4×10^{-3} mol) was added dropwise to a stirred solution of $[(cyclooctene)_2IrCl]_2$ (0.50 g, 5.6×10^{-4} mol) in 50 mL of tetrahydrofuran. After cooling to 0 °C, potassium *tert*-butylazapentadienide (0.27 g, 1.7×10^{-3} mol) was added dropwise, and the resulting solution was stirred at 0 °C for 20 min before evacuating to dryness. The orange residue was then extracted with pentane, filtered through Celite, and evacuated to dryness. The crude product (0.52 g, 9.6×10^{-4} mol) was dissolved in a minimal quantity of pentane. Cooling

(15) Bleeke, J. R.; Boorsma, D.; Chiang, M. Y.; Clayton, T. W., Jr.; Haile, T.; Beatty, A. M.; Xie, Y.-F. *Organometallics* **1991**, *10*, 2391.
(16) Barany, H. C.; Braude, E. A.; Pianka, M. *J. Chem. Soc.* **1949**, 1898.
(17) Herde, J. L.; Lambert, J. C.; Senoff, C. V. In *Inorganic Syntheses*; Parshall, G. W., Ed.; McGraw-Hill: New York, 1974; Vol. 15, pp 18–20.

to −30 °C produced yellow crystals of **1a**. Crystalline yield: 0.35 g, 58%. Anal. Calcd for $C_{17}H_{41}IrNP_3$: C, 37.48; H, 7.60. Found: C, 36.89; H, 7.70. ^1H NMR (C_6D_6, 22 °C): δ 7.41 (d, J_{H-H} = 9.3 Hz, 1, H4), 4.27 (br m, 1, H2), 2.17 (m, 1, H3), 1.30 (m, 1, H1), 1.23 (s, 27, PMe_3's), 1.17 (s, 9, *t*-Bu), 0.14 (m, 1, H1). $^{13}C\{^1H\}$ NMR (C_6D_6, 22 °C): δ 164.5 (s, C4), 56.0 (s, *t*-Bu tertiary C), 54.6 (s, C2), 42.5 (q, J_{C-P} = 7.5 Hz, C3), 29.9 (s, *t*-Bu CH_3's), 24.8 (m, PMe_3's), 19.3 (q, J_{C-P} = 7.5 Hz, C1). $^{31}P\{^1H\}$ NMR (C_6D_6, 22 °C): δ −55.4 (br s). $^{31}P\{^1H\}$ NMR (CD_2Cl_2, −90 °C): δ −48.9 (dd, J_{P-P} = 73.7, 18.4 Hz, 1), −52.8 to −55.0 (second-order multiplet, 2). IR (KBr pellet, cm^{-1}): 2963 (s), 2931 (m), 2900 (m), 2865 (w), 2818 (w), 2808 (w), 1621 (s), 1422 (m), 1358 (w), 1293 (w), 1278 (m), 1241 (w), 1213 (w), 1182 (w), 1150 (m), 964 (m), 936 (s), 894 (w), 827 (w), 815 (w), 709 (m), 675 (w), 663 (m).

Synthesis of (*anti*-η^3-*tert*-butylazapentadienyl)Ir(PMe_3)$_3$ (1b). A procedure similar to that described above for **1a** was employed, except that after addition of the potassium *tert*-butylazapentadienide, the solution was warmed to room temperature and stirred for 4 h. After evacuation to dryness, the orange residue was extracted with pentane and filtered through Celite. The solution was then evacuated to dryness and the crude product (0.49 g, 9.0×10^{-4} mol) was dissolved in a minimal quantity of pentane. Cooling to −30 °C produced yellow crystals of **1b**: crystalline yield 0.31 g, 51%. Anal. Calcd for $C_{17}H_{41}IrNP_3$: C, 37.48; H, 7.60. Found: C, 36.89; H, 7.70. ^1H NMR (C_6D_6, 22 °C): δ 7.11 (d, J_{H-H} = 8.7 Hz, 1, H4), 4.35 (q, J_{H-H} = 4.8 Hz, 1, H2), 3.89 (m, 1, H3), 1.45 (m, 1, H1), 1.25 (m, 1, H1), 1.31 (s, 9, *t*-Bu), 1.23 (s, 27, PMe_3's). $^{13}C\{^1H\}$ NMR (C_6D_6, 22 °C): δ 158.9 (s, C4), 55.2 (s, *t*-Bu tertiary C), 50.1 (s, C2), 46.9 (q, J_{C-P} = 6.3 Hz, C3), 30.2 (s, *t*-Bu CH_3's), 24.2 (m, PMe_3's), 15.4 (q, J_{C-P} = 8.0 Hz, C1). $^{31}P\{^1H\}$ NMR (C_6D_6, 22 °C): δ −55.3 (br s). $^{31}P\{^1H\}$ NMR (CD_2Cl_2, −90 °C): δ −46.6 (dd, J_{P-P} = 54.8, 15.5 Hz, 1), −49.2 (dd, J_{P-P} = 35.5, 15.5 Hz, 1), −56.0 (dd, J_{P-P} = 54.8, 35.5 Hz, 1). IR (KBr pellet, cm^{-1}): 2961 (s), 2923 (m), 2897 (m), 1607 (s), 1419 (m), 1355 (w), 1294 (w), 1279 (m), 1211 (w), 1181 (m), 960 (m), 933 (s), 848 (w), 818 (w), 713 (m), 676 (w), 666 (m).

Synthesis of *fac*-$CH_2CH(CH_2C(O)CH_3)CH(CHNC(CH_3)_3)Ir(PMe_3)_3(H)\cdot{}^1/_2H_2O$ (2). Compound **1a** (0.52 g, 9.6×10^{-4} mol) was dissolved in a minimal quantity of acetone and cooled to −30 °C, causing **2** to crystallize as light yellow blocks: yield 0.35 g, 60%. Anal. Calcd for $C_{20}H_{48}IrNO_{1.5}P_3$: C, 39.26; H, 7.92. Found: C, 39.28; H, 7.71. ^1H NMR (CD_2Cl_2, 22 °C): δ 7.36 (d, J_{H-H} = 8.5 Hz, 1, H4), 2.95 (m, 1, H2), 2.09 (m, 2, acetone CH_2's), 1.98 (s, 3, acetone CH_3's), 1.63 (m, 1, H3), 1.46 (d, J_{H-P} = 7.3 Hz, 9, PMe_3), 1.38 (m, 18, PMe_3's), 1.04 (s, 9, *t*-Bu), 0.73 (m, 1, H1), −0.35 (m, 1, H1), −10.80 (d of t, J_{H-P} = 152, 18 Hz, 1, Ir–H). $^{13}C\{^1H\}$ NMR (CD_2Cl_2, 22 °C): δ 209.2 (s, C=O), 174.9 (s, C4), 62.3 (s, acetone CH_2), 54.8 (s, *t*-Bu tertiary C), 49.0 (s, C2), 30.9 (s, acetone CH_3), 29.9 (s, *t*-Bu CH_3's), 22.7 (m, PMe_3), 18.3 (m, PMe_3's), 1.72 (d, J_{C-P} = 61.6 Hz, C3), −26.6 (d, J_{C-P} = 61.6 Hz, C1). $^{31}P\{^1H\}$ NMR ($(CD_3)_2CO$, 22 °C): complex second-order ABC pattern centered at δ −51.7. IR (KBr pellet, cm^{-1}): 3346 (w), 2965 (s), 2904 (s), 2818 (m), 1972 (s), 1699 (s), 1611 (s), 1435 (w), 1420 (m), 1369 (w), 1353 (m), 1302 (m), 1285 (s), 1247 (w), 1212 (w), 1124 (w), 1093 (w), 1080 (w), 963 (s), 940 (s), 869 (m), 855 (m), 721 (m), 681 (w), 670 (m), 568 (w).

Synthesis of (η^4-CH_2=CHCH=$CH(NHC(CH_3)_3)$)Ir(PMe_3)$_3$$^+O_3SCF_3^-$ (3). Compound **1b** (0.20 g, 3.7×10^{-4} mol) was dissolved in 20 mL of diethyl ether and cooled to −30 °C. Cold (−30 °C) triflic acid (0.055 g, 3.7×10^{-4} mol) was then added, and the resulting solution was stirred briefly before storing at −30 °C. Overnight, orange solid precipitated from solution. The supernatant was decanted off, and the solid was washed with pentane and ether before drying under vacuum for 2 h: crude yield 0.24 g, 3.4×10^{-4} mol. Crystals of **3** were obtained by dissolving in minimal acetone and cooling to −30 °C: crystalline yield 0.15 g, 58%. Anal. Calcd for $C_{18}H_{42}F_3IrNO_3P_3S$: C, 31.11; H, 6.11. Found: C, 30.73; H, 6.12. ^1H NMR ($(CD_3)_2CO$, −20 °C): δ 5.11 (m, 1, H3), 4.94 (m, 1, H2), 2.38 (m, 1, H4), 1.80 (d, J_{H-P} = 9.7 Hz, 9, PMe_3), 1.71 (d, J_{H-P} = 9.2 Hz, 9, PMe_3), 1.58 (d, J_{H-P} = 9.2 Hz, 9, PMe_3), 1.55 (m, 1, H1), 1.07 (s, 9, *t*-Bu), 1.02 (m, 1, N–H), −0.11 (m, 1, H1). $^{13}C\{^1H\}$ NMR ($(CD_3)_2CO$, −20 °C): δ 82.9 (s, C3), 76.2 (s, C2), 65.9 (d, J_{C-P} = 40.9 Hz, C4), 52.9 (s, *t*-Bu tertiary C), 28.9 (s, *t*-Bu CH_3's), 26.8 (d, J_{C-P} = 33.8 Hz, C1), 21.1 (d, J_{C-P} = 34.3 Hz, PMe_3), 20.2 (d, J_{C-P} = 32.3 Hz, PMe_3), 19.7 (d, J_{C-P} = 33.6 Hz, PMe_3). $^{31}P\{^1H\}$ NMR ($(CD_3)_2CO$, −20 °C): δ −44.7 (d, J_{P-P} = 18.1 Hz, 1), −48.6 (dd, J_{P-P} = 22.8, 18.1 Hz, 1), −51.1 (d, J_{P-P} = 22.8 Hz, 1). IR (KBr pellet, cm^{-1}): 2968 (s), 2910 (m), 2867 (w), 1430 (m), 1363 (w), 1309 (w), 1293 (m), 1203 (w), 1067 (w), 947 (s), 843 (s), 728 (m), 675 (w), 557 (m).

Treatment of Compound 1a with Triflic Acid. Synthesis of a Mixture of Compound 3 and (*syn*-η^3-*tert*-butylazapentadienyl)Ir(PMe_3)$_3$(H)$^+O_3SCF_3^-$ (4). In an NMR tube, compound **1a** was dissolved in CD_2Cl_2, and 1 equiv of triflic acid was added. NMR spectra showed the presence of an 80/20 mixture of compound **3** (*vide supra*) and compound **4**. Selected spectroscopic data for **4**: ^1H NMR (CD_2Cl_2, 22 °C) δ 7.38 (d, J_{H-H} = 9.8 Hz, 1, H4), 5.58 (m, 1, H2), 2.96 (m, 1, H3), 2.90 (br s, 1, H1), 1.80 (br s, 1, H1), −15.17 (d of t, J_{H-P} = 129.4, 17.1 Hz, 1, Ir–H); $^{31}P\{^1H\}$ NMR (CD_2Cl_2, 22 °C) δ −46.9 (d, J_{P-P} = 12.1 Hz, 1), −47.6 (d, J_{P-P} = 18.2 Hz, 1), −55.2 (dd, J_{P-P} = 18.2, 12.1 Hz, 1).

Synthesis of [(η^4-CH_2=CHCH=$CH(NH_2C(CH_3)_3)$)Ir(PMe_3)$_3$]$^{2+}$ ($O_3SCF_3^-$)$_2$ (5). Compound **3** (0.20 g, 2.9×10^{-4} mol) was dissolved in 20 mL of acetone and treated with triflic acid (0.043 g, 2.9×10^{-4} mol). The volatiles were then removed under vacuum, and the remaining yellow solid (compound **5**) was washed with diethyl ether: yield 0.22 g, 90%. Anal. Calcd for $C_{19}H_{43}F_6IrNO_6P_3S_2$: C, 27.01; H, 5.14. Found: C, 27.00; H, 5.41. ^1H NMR ($(CD_3)_2CO$, 22 °C): δ 7.40, 7.25 (br s's, 2, N–H's), 5.87 (m, 1, H3), 5.41 (m, 1, H2), 2.18 (m, 1, H1), 1.93 (d, J_{H-P} = 10.1 Hz, 9, PMe_3), 1.81 (m, 1, H4), 1.80 (d, J_{H-P} = 9.2 Hz, 9, PMe_3), 1.72 (d, J_{H-P} = 9.8 Hz, 9, PMe_3), 1.47 (s, 9, *t*-Bu), 0.28 (m, 1, H1). $^{13}C\{^1H\}$ NMR ($(CD_3)_2CO$, 22 °C): δ 82.7 (s, C3), 81.8 (s, C2), 64.6 (s, *t*-Bu tertiary C), 48.0 (d, J_{C-P} = 51.0 Hz, C4), 32.5 (d, J_{C-P} = 32.9 Hz, C1), 25.1 (s, *t*-Bu CH_3's), 22.4 (d, J_{C-P} = 34.6 Hz, PMe_3), 21.5 (d, J_{C-P} = 32.1 Hz, PMe_3), 20.1 (d, J_{C-P} = 36.1 Hz, PMe_3). $^{31}P\{^1H\}$ NMR ($(CD_3)_2CO$, 22 °C): δ −42.5 (s, 1), −49.3 (d, J_{P-P} = 26.6 Hz, 1), −54.5 (d, J_{P-P} = 26.6 Hz, 1). IR (KBr pellet, cm^{-1}): ~3400 (w), 3068 (w), 2988 (w), 2925 (w), 1430 (w), 1385 (w), 1314 (m), 1287 (s), 1241 (s), 1225 (s), 1162 (m), 1030 (s), 972 (w), 948 (m), 864 (w), 735 (w), 637 (s), 574 (w), 517 (w).

Treatment of the Mixture of Compounds 3 and 4 with Triflic Acid. Synthesis of a Mixture of Compound 5 and [(*syn*-η^3-CH_2–CH–CHCH=$NHC(CH_3)_3$)Ir(PMe_3)$_3$(H)]$^{2+}$($O_3SCF_3^-$)$_2$ (6). In an NMR tube, the 80/20 mixture of compounds **3** and **4** in CD_2Cl_2 was treated with an additional 1 equiv of triflic acid. NMR spectra showed the presence of an 80/20 mixture of compound **5** (*vide supra*) and compound **6**. Selected spectroscopic data for **6**: ^1H NMR (CD_2Cl_2, 22 °C) δ 11.70 (br s, 1, N–H), 8.40 (m, 1, H4), 6.45 (m, 1, H2), 3.41 (m, 1, H3), 3.11 (br s, 1, H1), 2.35 (br s, 1, H1), −13.90 (d of t, J_{H-P} = 128.7, 16.8 Hz, 1, Ir–H); $^{31}P\{^1H\}$ NMR (CD_2Cl_2, 22 °C) δ −40.1 (dd, J_{P-P} = 8.6, 6.7 Hz, 1), −48.0 (dd, J_{P-P} = 18.9, 6.7 Hz, 1), −54.4 (dd, J_{P-P} = 18.9, 8.6 Hz, 1).

X-ray Diffraction Studies of *fac*-$CH_2CH(CH_2C(O)CH_3)CH(CHNC(CH_3)_3)Ir(PMe_3)_3(H)\cdot{}^1/_2H_2O$ (2) and (*anti*-η^3-*tert*-butylazapentadienyl)Ir(PMe_3)$_3$ (1b). Single crystals of **2** and **1b** were sealed in glass capillaries under an inert atmosphere. Data were collected at room temperature, using graphite-monochromated Mo Kα radiation. Standard reflections were measured every 100 events as check reflections for crystal deterioration and/or misalignment. All data reduction and refinement were done using the Siemens SHELXTL PLUS package on a Vax 3100 workstation.[18] Crystal data and details of data collection and structure analysis are listed in Table 5.

The iridium atom positions in **2** and **1b** were determined by direct methods. In each case, the remaining non-hydrogen atoms

(18) Atomic scattering factors were obtained from the following: *International Tables for X-Ray Crystallography*; Kynoch Press: Birmingham, England, 1974; Vol. IV.

Table 5. X-ray Diffraction Structure Summary

	2	1b
Crystal Parameters and Data Collection Summary		
formula	$C_{20}H_{48}IrNO_{1.5}P_3$	$C_{17}H_{41}IrNP_3$
fw	611.7	544.6
cryst syst	monoclinic	monoclinic
space group	$C2/c$	$P2_1/n$
a, Å	31.117(6)	15.709(14)
b, Å	11.104(2)	26.154(10)
c, Å	18.457(5)	18.915(7)
α, deg	90.0	90.0
β, deg	119.26(2)	108.97(3)
γ, deg	90.0	90.0
V, Å^3	5563(2)	7351(3)
Z	8	12
cryst dimens, mm	0.10 × 0.40 × 0.20	0.40 × 0.18 × 0.50
cryst color and habit	yellow cube	yellow plate
calcd density, g/cm^3	1.461	1.476
radiation, Å	Mo Kα, 0.710 73	Mo Kα, 0.710 73
scan type	ω	ω
scan rate, deg/min in ω	variable; 3.50–14.65	variable; 3.50–14.65
scan range (ω), deg	1.20	1.20
2θ range, deg	3.0–50.0	3.0–50.0
data collected	h, 0–36; k, 0–13; l, −21 to +18	h, 0–18; k, 0–31; l, −22 to +21
total decay	none detected	none detected
temp, K	295	295
Treatment of Intensity Data and Refinement Summary		
no. of data collected	5260	13 709
no. of unique data	4877	12 885
no. of data with $I > 3\sigma(I)$	2890	7011
Mo Kα linear abs coeff, cm^{-1}	49.84	56.43
abs cor applied	semiempirical	semiempirical
data to param ratio	11.8:1	11.8:1
R^a	0.033	0.053
$R_w{}^a$	0.042[b]	0.069[c]
GOF[d]	1.00	0.98

[a] $R = \sum\|\|F_o\| - \|F_c\|\|/\sum\|F_o\|$. $R_w = [\sum w(\|F_o\| - \|F_c\|)^2/\sum w\|F_o\|^2]^{1/2}$. [b] $w = [\sigma^2(F_o) + 0.0009F_o^2]^{-1}$. [c] $w = [\sigma^2(F_o) + 0.0031F_o^2]^{-1}$. [d] GOF $= [\sum w(\|F_o\| - \|F_c\|)^2/(N_{observations} - N_{variables})]^{1/2}$.

were found by successive full-matrix least-squares refinement and difference Fourier map calculations. All non-hydrogen atoms were refined anisotropically, while the metal-bound hydrogen atom in **2** was refined isotropically. All other hydrogens in **2** and **1b** were placed at idealized positions and assumed the riding model. In each case, a common isotropic U value for all hydrogens was refined.

Dynamic NMR Studies. Determination of $\Delta G^\ddagger$. Theoretical line shapes were calculated for a series of rates using the method of Johnson.[19,20] The experimental spectra were matched against the theoretical spectra and, in this way, exchange rate constants were determined for each temperature. These exchange rate constants, k, were then used to calculate the free energy of activation, $\Delta G^\ddagger$, at each temperature, T, using the Eyring equation.[21] The reported $\Delta G^\ddagger$ is the average value over all of the temperatures in the simulation and the uncertainty is the estimated standard deviation.

Acknowledgment. We thank the National Science Foundation (Grants CHE-9003159 and CHE-9303516) and the donors of the Petroleum Research Fund, administered by the American Chemical Society, for support of this research. A loan of $IrCl_3 \cdot 3H_2O$ from Johnson-Matthey Alfa/Aesar is gratefully acknowledged. Washington University's X-ray Crystallography Facility was funded by the National Science Foundation's Chemical Instrumentation Program (Grant CHE-8811456). The High Resolution NMR Service Facility was funded in part by National Institutes of Health Biomedical Support Instrument Grant 1 S10 RR02004 and by a gift from Monsanto Co.

Supplementary Material Available: Tables of structure determination summaries, final atomic coordinates, thermal parameters, bond lengths, and bond angles for compounds **2** and **1b** and ORTEP drawings for crystallographically independent molecules 2 and 3 of compound **1b** (23 pages). Ordering information is given on any current masthead page.

OM930733A

(19) Johnson, C. S., Jr. *Am. J. Phys.* **1967**, *35*, 929.
(20) Martin, M. L.; Martin, G. J.; Delpuech, J.-J. *Practical NMR Spectroscopy*; Heydon: London, 1980; pp 303–309.
(21) Lowry, T. H.; Richardson, K. S. *Mechanism and Theory in Organic Chemistry*; Harper and Row: New York, 1976.